Influence of electricity prices on energy flexibility of integrated hybrid heat pump and thermal storage systems in a residential building

Peter Fitzpatrick[a], Francesco D'Ettorre[a], Mattia De Rosa[a,b,*], Malcolm Yadack[c], Ursula Eicker[d], Donal P. Finn[a,b]

[a]*School of Mechanical and Materials Engineering, University College Dublin. Ireland*
[b]*UCD Energy Institute, University College Dublin. Ireland*
[c]*School of Applied Science Stuttgart. Stuttgart, Germany*
[d]*Gina Cody School of Engineering and Computer Science, Concordia University. Montréal, Canada*

Abstract

The aim of the present paper is to investigate the influence of electricity tariffs on energy flexibility in buildings and associated energy costs. A residential building located in Stuttgart, Germany, equipped with a hybrid heat pump which is coupled with a thermal energy storage unit and a gas boiler is used as a case study. A model predictive control algorithm is used to minimise the daily operational cost over a full heating season. Several demand response programs based on controlling the heat pump power consumption were tested and analysed by adopting different metrics capable of describing the flexibility potential and cost of demand response programs. Several tariff structures, including: real-time pricing, two-level day-night tariffs and critical-peak pricing with both fixed and variable feed-in price components, were investigated. The results show that the building can provide up to 1370 kWh_e of energy flexibility over the heating season with an average specific (marginal) costs of between €0.024 - 0.035 per kWh_e of flexibility provided. The demand response programs lead to higher utilisation of thermal energy storage along with increased boiler consumption, by up to 17.1% and 12.1%, respectively in case of maximum demand response intensity. This in turn leads to a higher overall primary energy consumption of between 1.6% and 9.1% depending on demand response intensity. Typically, real-time pricing is the most favourable tariff structure, capable of offering the greatest energy flexibility with lowest associated electricity costs.

Keywords: buildings, demand response, tariffs, flexibility, heat pumps, thermal storage, optimised control

*Corresponding author

Email addresses: peter.fitzpatrick.2@ucdconnect.ie (Peter Fitzpatrick), francesco.dettorre@gmail.com (Francesco D'Ettorre), mattia.derosa@ucd.ie (Mattia De Rosa), malcolm.yadack@hft-stuttgart.de (Malcolm Yadack), ursula.eicker@concordia.ca (Ursula Eicker), donal.finn@ucd.ie (Donal P. Finn)

1. Introduction

As part of the European Union Climate and Energy initiative for 2030, binding legislation has been put in place to ensure that climate and energy targets (i.e., 40% cut in GHG emissions from 1990 levels, 27% of EU energy from renewable sources and a 27% improvement in energy efficiency) [1] are met. As part of these targets, there is a need for electricity grids to incorporate a greater amount of renewable power with generation assets, thereby allowing them to increase their share of low carbon electricity generation and, consequently, to reduce their carbon footprint. However, the aleatory nature of renewable energy sources can pose substantial challenges from the perspectives of grid stability and management [2]. Reliable operation of the grid requires a perfect balance between supply and demand at all times. This is usually achieved by adjusting the energy generated in order to meet the demand [3]. However, the flexibility offered by traditional power systems may be not sufficient to cope with uncertainties in both demand and generation in the case of high penetration of renewable energy sources [4]. Therefore, new flexibility resources to improve the elasticity of the power system need to be identified and incorporated with the grid.

A paradigm shift towards a future electrical system, in which end-users become a key element for providing the flexibility required by the national grid, is currently undergoing [5]. Even though the participation of end-users can result in higher complexity of system management, it may have a positive impact on mitigating the volatility of electricity prices [6]. In this scenario, new smart technologies and advanced control systems can enable *demand side management* (DSM) strategies aiming to reduce, optimise and adapt end-user energy consumption depending on specific dynamic contexts. In particular, demand response (DR) programs represent a promising technique for the emerging smart grid frameworks, based on the voluntary modification of consumer load profiles through direct external requests [7].

DR programs can play an increasingly important role in both reducing short-term electricity pricing and in deferring capacity and grid investments. Su and Kirschen [8] showed that increasing levels of demand shifting can lead to a reduction of market clearing prices, benefiting all bidders even if they do not participate in shifting activities. It also outlined that demand shifting improves the economic efficiency of the day-ahead market as the effective serving system cost tends to decrease. Also, a substantial saving in the system operating cost is transferred to the demand side with increasing levels of shifting. Generally, the benefits of enabling DR programs can be summarised as shown in Table 1 [6].

Demand Response has seen several implementations over the last few decades. The simplest example is represented by the *Time of Use* (ToU) tariffs under which a consumer is subjected by different price levels during peak to off-peak periods [9]. The overall objective is to encourage energy use during off-peak hours by setting lower prices compared to high peak hours [10]. Similarly, *Critical Peak Pricing* is another type of DR program where significantly higher prices are charged, typically with very short notice, if the grid becomes stressed. Both the above schemes fall into the *Price-based DR programs* category in which the DR action is driven by a passive economic motivation [11]. Another category is represented by the *Incentive-based DR Programs* in which direct incentives paid to the end user in return of load reduction triggered by an external request. Examples of these measures are: Direct

Table 1: Recognised benefits from DR programs [6].

Dimension	**Benefits**
End-users & Prosumers	- Energy consumption optimisation. - Cash flow revenue from incentive payments. - Long-term bill savings. - Improved thermal comfort through smart technologies. - Improved energy-related awareness among customers.
Market & Infrastructure	- Flexible load demand pattern. - Creating a *load follow supply* strategy. - Diversification of energy resources. - Avoided/deferred infrastructure costs. - Reduced market power. - Reduction of energy prices at grid level. - Overloads reduction in the distribution system.
Environment	- Reduction of carbon emission at grid level. - Rational usage of energy resources. - Higher renewable penetration.

load control, Demand side bidding, Capacity markets, etc. [4].

Generally, end-user ability to control the demand in response to electrical grid requirements strictly depends on their type and size. Typically, industrial and large commercial settings are particularly suitable for DR activation, due to the magnitude of their power demands and for being often already equipped with the systems and facilities required for enabling DR programs [12]. Notwithstanding, residential and commercial end-users represent an interesting potential source of energy flexibility for the electricity network [13], being the building sector responsible for about 36% and 40% of the overall energy use and carbon emissions worldwide, respectively [14]. Proposals for new residential buildings equipped with connected sensors and smart controllers responsive to smart grid signals have been proposed and analysed over the last few years [15–18].

Several residential systems can be exploited for activating DR programs, such as domestic appliances (i.e., washing machines, dryer, dishwashers, etc.), heating/cooling systems (i.e., heat pumps, electric resistance heating) and onsite generation systems (i.e., solar thermal/PV panels, combined heat and power systems, etc.). As for instance, Chassin et al. [19] showed that elasticity in energy demand for heating/cooling purposes up to 25% can be achieved by controlling and optimising the load on the base of real-time prices or time of use tariffs. Similarly, Pallonetto et al. [20] tested rule-based and predictive control algorithms to optimise DR strategies under different ToU tariff structures in an all-electric residential building equipped with a geothermal heat pump system, solar photovoltaic (PV) panels, thermal solar collectors and thermal storage. The results showed that significant savings can be obtained in terms of utility generation cost (up to 20.5% and 41.8% for rule-based and predictive algorithm, respectively) and carbon emission (up to 18.8% and 39% for rule-based and predictive algorithm, respectively).

Despite this promising framework, several barriers still limit a widespread development of DR programs in residential buildings. Due to the fact that DR represents an intentional change in electricity usage due to price fluctuations or incentive payments, the impact of the consumer behaviour strongly affects the benefits of DR programs. Consumers who exhibit more variable load patterns on normal days may be capable of altering their loads more significantly in response to dynamic pricing plans [21]. On the other hand, customer behaviour will unlikely change as a result of DR implementation, since the daily economic benefit from the DR activation may be of little financial incentive to the end users. This is why the majority of DR programs use information technology to develop automated systems for managing end-use participation [20]. Aggregating flexibility profiles of multiple end-users could smooth the uncertainties associated with user behaviour [22]. Notwithstanding, the absence of appropriate market mechanisms, the complexity of available price structures, administrative overhead associated with contractual forms, consumer inertia, all still represent a challenge for the access of residential end users to DR markets [23–25].

Compounding this research gap is the lack of harmonised procedures and formalised standards to assess the energy flexibility of DR programs in residential buildings [26]. Recent efforts towards establishing a common terminology to characterise DR programs at building level has been carried out by the IEA EBC Annex 67 [27], which developed an evaluation framework based on three aspects of the building energy flexibility: capacity, duration and cost. Flexibility potential is calculated by evaluating the capability of buildings to dynamically change their demand profiles according to external penalty signals, such as energy prices, carbon emissions, etc. [28]. However, understanding the flexibility potential requires appropriate and measurable metrics which can be communicated and easily interpreted among different stakeholders and capable of capturing the different technical and economic aspects of DR programs.Furthermore, the influence of the market context - reflected by market prices, tariffs and contractual agreements - represents a continuing challenge that needs to be addressed for complete assessment of DR potential at an aggregate level. This is a prerequisite for subsequent extension of the analysis to portfolios of building flexibility assets for market operators and, in turn, to understand the influence of such portfolios at a market level. Linking these market and regulatory issues with the task of improving accessibility for end users continues to present challenges towards enabling the deployment of DR technologies in buildings [4].

In order to address these challenges, the aim of the present paper is to investigate the influence of energy market frameworks on building flexibility and associated energy performance and costs. A residential building, located in Wüstenrot, Stuttgart, Germany and serving as a demonstration site of the H2020 Sim4Blocks project, is selected as case study. The building is a three-storey residential building equipped with a hybrid heat pump (HP) coupled with a thermal energy storage (TES) and a gas boiler (Section 2.1). An EnergyPlus model was developed and validated against experimental data from previous work, where a top-down methodology to reduce the complexity of building thermal resistance capacitance (RC) network models was tested in order to detect a trade-off between accuracy and computational costs. [29]. The resulting reduced-order RC model detected by the trimming procedure is used in the present work to simulate the building thermal behaviour (Section

2.2). A model predictive controller in MATLAB is used to minimise the daily operational cost over the heating season (Section 2.3). Several DR programs based on controlling the HP power consumption were tested and analysed under different electricity pricing tariffs, such as hourly real time prices and time-of-use tariffs (Section 2.5). The DR programs assessment is carried out by introducing several metrics capable of describing the flexibility potential and associated cost of the measures adopted (Section 2.4). Finally, Section 3 and Section 4 reports the results and conclusions obtained by the presented analysis.

2. Materials and methods

A model predictive controller, implemented in MATLAB, optimises the control of the heat pump and gas boiler for each day based on the thermal load and the electricity price during the day. As the model can predict the behaviour of the building temperature, the heating load can be optimised for each day in terms of cost. Different electricity prices are used for the various DR measures. This allows the effect of different electricity prices to be analysed. The different prices used are a typical two-level tariff, which can be used for a baseline comparison, various time-of-use tariffs and RTP, where different cost components are considered. DR measures vary with the magnitude of electricity reduced during the DR event, the intensity, and the duration of the DR events. Furthermore, the analysis examines the technical implications and economic aspects due to the various DR measures. A schema of the approach utilised is provided in Figure 1.

2.1. Reference building

A three-storey residential building (Figure 2), with a living area of 310 m^2, was selected to test several demand response programs. The building is part of a plus energy district, located in Wüstenrot, Stuttgart, Germany and serving as a demonstration site of the H2020 Sim4Blocks project, consisting of 17 newly built highly energy efficient residential buildings served by a geothermal water network. The considered building is equipped with a brine/water heat pump (22 kW thermal output) and two buffer storage tanks (1000 litres for space heating and 400 litres for DHW). Detailed monitoring data, with time intervals of 30 seconds, were available for all relevant thermal and electrical energy consumption, as well as for internal building zone temperatures and weather conditions (i.e., ambient temperature and solar radiation). Table 2 reports the main geometric characteristics of the building, more details can be found in [29].

The building thermal demand is provided by a hybrid system, consisting of an air-to-water heat pump (HP), a gas boiler and the hot water tank used as thermal energy storage (TES). In accordance with the user preference, the comfort period is defined between 8 am - 9 pm with the thermostatic set-point T_{room}^{SP} set to 22^oC, while no heating is scheduled outside this time period, unless the indoor temperature dropped below 15^oC. During the operating hours, the building thermal demand requested by the building can be met by the boiler, the heat pump and/or the TES. A Model Predictive Controller (MPC) is used to optimise the system schedule, as described in the following sections.

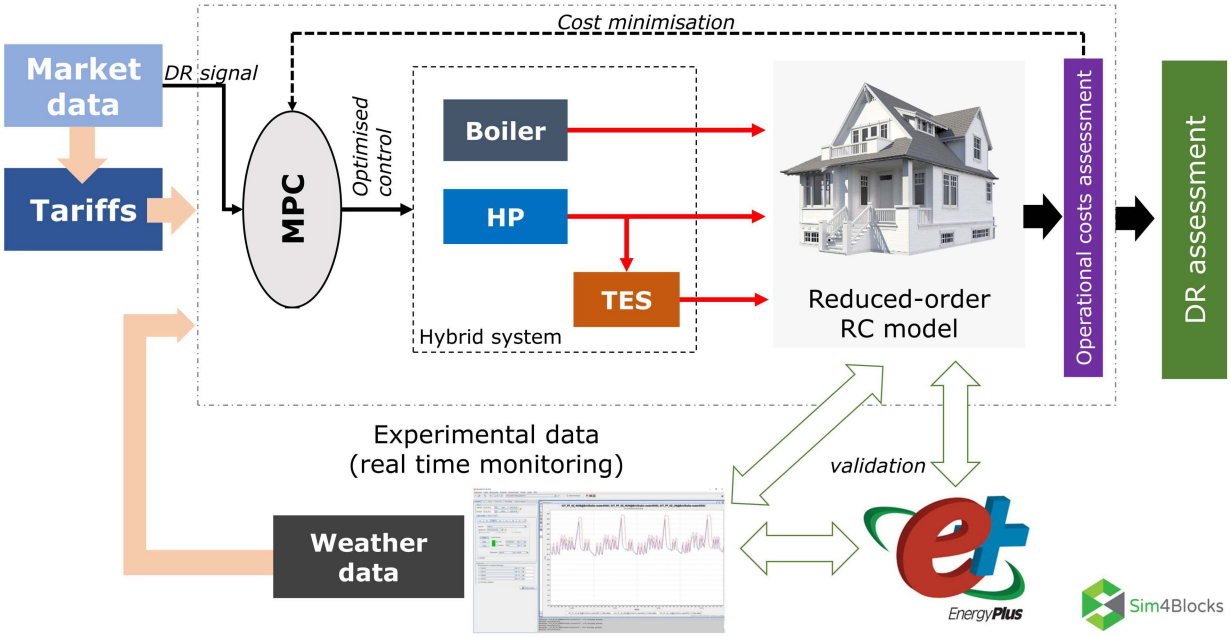

Figure 1: Schematic of the methodology adopted. Notes: (i) the reference building is described in section 2.1; (ii) experimental data and building model validation are reported in De Rosa et al. [29]; (iii) the hybrid system model is fully described in section 2.3; (iv) market data and the tariff structures are summarised in section 2.5, while a detailed description can be found in Schmidt et al. [30]; (v) the DR signal is equal to 0 for the baseline scenario (no DR activated).

2.2. Building modelling

An EnergyPlus model was developed and validated against experimental data in a previous work [29], where a top down methodology to reduce the complexity of building thermal network (RC) models [31] was analysed in order to examine the trade off between accuracy and computational costs. The resulting reduced-order RC model as determined by the trimming procedure is used in the present work to simulate the building thermal behaviour (see section 2.3). More details about the types of building models developed, the calibration procedure performed and the results obtained can be found in [29].

The building dynamic is therefore described by a linear state-space model in which the general relationship between state variables ($\mathbf{x}$) and control variables ($\mathbf{u}$) is shown in Eq. 1. The matrices A and B represent the state and the input matrices, respectively. The state vector $\mathbf{x}$ consists of the node temperatures, with $\mathbf{u}$ being the input vector containing the input signals, thermal power delivered to the building by the generation system and weather conditions.

$$x_{k+1} = Ax_k + Bu_k \tag{1}$$

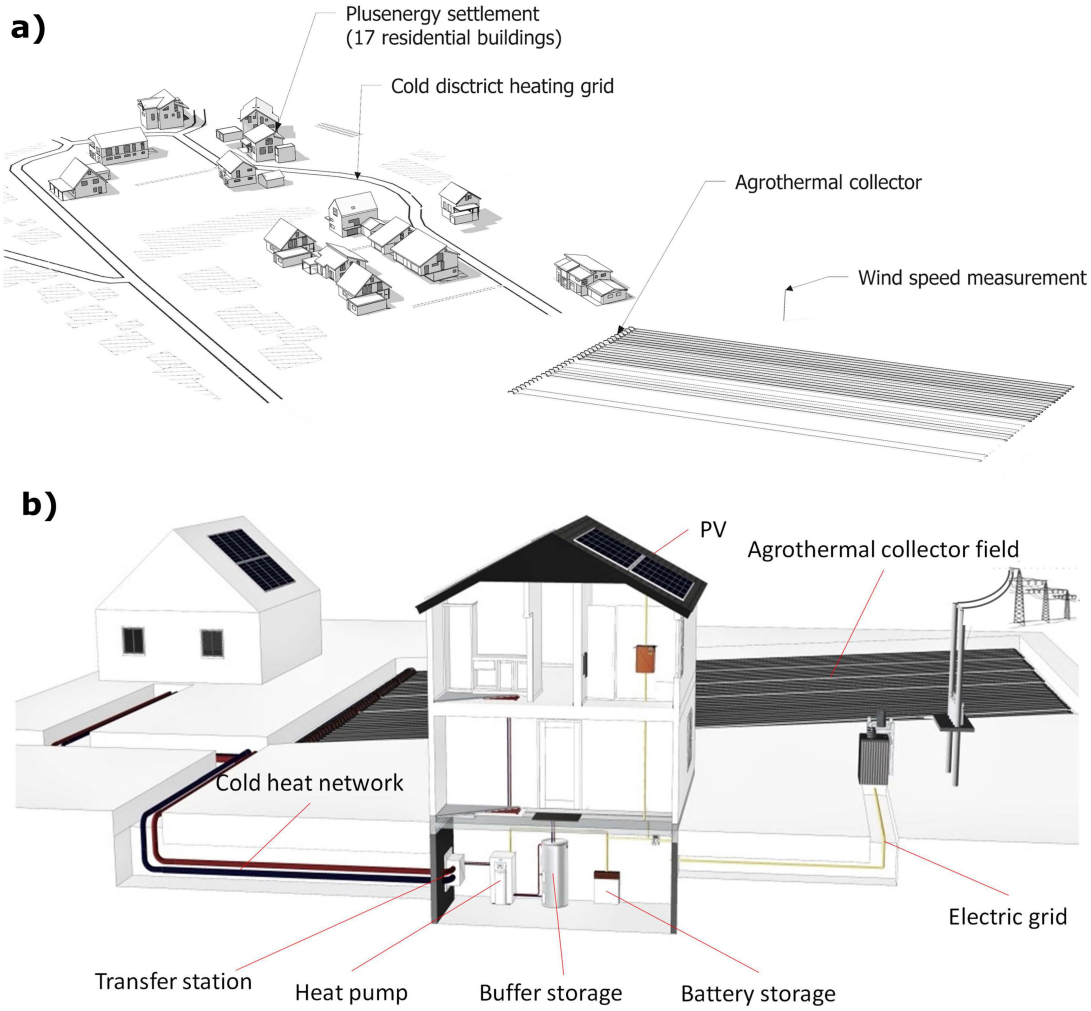

Figure 2: a) Sim4Blocks pilot site located in Wüstenrot, Germany. b) Schematic of the considered building. [29]

2.3. Hybrid system modelling

The hybrid system is intended to be operated with the objective of minimising the energy bill, while maintaining indoor temperature at acceptable levels. Therefore, a Model Predictive Control (MPC) algorithm is implemented to optimise the fuel switching strategy between the heat pump and the gas boiler, while also exploiting the best times during the day for charging/discharging the TES, thus minimising the overall system operating costs. The optimal control problem is formulated as a mixed-integer linear programming problem (MILP) and implemented in MATLAB through the use of the YALMIP toolbox, while the IBM CPLEX is used as a solver [32].

The heat pump and gas boiler can be operated either independently or simultaneously. However, only the heat pump can be operated to charge the TES, and during the charging phases, it cannot satisfy the load demand. The HP is modelled by the second-law efficiency

Table 2: Building geometry [29]

Parameter		**Value/Range**
Latitude		49.6° North
Longitude		9.6° East
Elevation		495 m
Number of storeys		3
External walls	North	109.9 m^2
	South	147.3 m^2
	East	84.5 m^2
	West	85.0 m^2
	Basement	139.9 m^2
	Flat roof	25.0 m^2
	Tilted roof (South)	46.9 m^2
	Tilted roof (North)	78.9 m^2
Windows	North	36.5 m^2
	South	28.6 m^2
	East	5.2 m^2
	West	13.0 m^2
Solar heat gain coefficient		0.583
Roof pitch		15°
Envelope leakage (ACH)		0.3 1/h
Wall absorptance		0.2 (white)

expression as shown in Eq. 2, where T_{sink} and T_{source} are the sink and source temperatures which are set equal to the external temperature and heat supply temperature, respectively. This approach has been shown to be an effective way to model heat pump performance, while keeping a low model complexity, so as to ensure a high computational speed [33]. If the HP directly meets the load, the supply temperature is considered equal to that required by the emission system. In the case of the HP being used to charge the TES, the supply temperature is considered equal to the maximum storage temperature.

$$COP = \eta^{II} \frac{T_{sink}}{T_{sink} - T_{source}} \tag{2}$$

The gas boiler is modelled with a constant efficiency (i.e., $\eta_{boiler} = 0.96$) over its operational range, while the water tank is modelled as a perfectly-mixed tank with a nominal temperature of 45 ^oC, using the following energy balance:

$$\rho V c \frac{dT_{TES}}{d\tau} = \dot{Q}_{HP,TES} - \dot{Q}_{TES,L} - \dot{Q}_{loss} \tag{3}$$

Technological constraints are introduced by limiting the minimum and maximum thermal outputs that can be provided by the two generators, as well as the maximum amount of

useful energy ($E_{TES,useful}$) that can be taken from the TES (see Eqs. 4-6).

$$\dot{Q}_{HP}^{min} \leq \dot{Q}_{HP} \leq \dot{Q}_{HP}^{max} \tag{4}$$

$$0 \leq \dot{Q}_{B} \leq \dot{Q}_{B}^{max} \tag{5}$$

$$0 \leq Q_{TES,L} \leq E_{TES,useful} \tag{6}$$

As it is not desired that the heat pump is operational when its load factor drops below a minimum percentage of its nominal value, the thermal power becomes a semi-continuous variable, taking the following form:

$$Z_{HP}^{L} = \phi_{HP}^{L} \dot{Q}_{HP}^{L} \tag{7}$$

As the optimisation problem is solved by means of mixed-integer linear programming, Eq. 7 has to be linearised. This can be done by introducing the following inequality constraints:

$$\phi_{HP}^{L} \cdot Q_{HP,L}^{min} \leq Q_{HP,L} \leq \phi_{HP}^{L} \cdot Q_{HP,L}^{max} \tag{8}$$

$$Q_{HP,L}^{min} \ (1 - \phi_{HP}^{L} \ ) \leq z_{HP}^{L} - Q_{HP,L} \leq Q_{HP,L}^{max} \ (1 - \phi_{HP}^{L}) \tag{9}$$

In order to examine some initial DR measures, the following parameters are considered:

$$\alpha_{DR} = \frac{P_{HP}^{DR}}{P_{HP}^{ref}} \tag{10}$$

$$\tau_{DR} = l \Delta t_{DR}^{min} \tag{11}$$

The term P_{HP}^{DR} and P_{HP}^{ref} in Eq. 10 represent the HP power consumption after the implementation of the DR measure and for the no DR baseline case, respectively. Therefore, α can be a value between 0 and 1, with $(1 - \alpha)$ being the amount of electric power reduced or, equivalently, the intensity of the DR measure. The parameter l represents the duration of the DR measure, ranging from its minimum duration ($\Delta t_{DR}^{min} = 15m$) for $l = 1h$, to a maximum of 4 hours when $l = 16h$.

The hourly electricity price is used as an external signal to simulate the request of DR actions from the grid. When the electricity price is higher than an upper threshold value, the reference heat pump consumption is reduced to a fraction specified by α. The upper threshold value is calculated for each day by obtaining the standard deviation of electricity prices for that day. A lower threshold is also calculated which can be used for charging the thermal energy storage during times of low electricity price. For each scenario, an optimum control strategy is defined by solving a new OCP in which the objective function is the same adopted in the baseline case, with new constraints added to account for the DR actions.

The aim of the controller is to minimise the daily operational cost of the system while preserving the comfort condition of the building. The objective function is defined as the sum of hourly operational costs over the whole day (Eq. 12).

$$C_{op}^{Day} = \int_0^T [p_{el} \cdot (\psi_{HP,TES} \cdot \frac{\dot{Q}_{HP,TES}}{COP_{TES}} + \psi_{HP,L} \cdot \frac{\dot{Q}_{HP,L}}{COP_L}) + p_{gas} \cdot \frac{\dot{Q}_B}{\eta_B}]dt \tag{12}$$

2.4. Flexibility metrics

The lack of common and standardised assessment procedures to evaluate DR programs is still one of the main challenges to unlock energy flexibility in buildings. Establishing standardised key performance indicators (KPI) for DR programs is paramount to enable a communication channel between the different stakeholders [27]. In the present work, three indicators have been selected to assess the building flexibility potential from a technical, economic and energy performance point of view:

- Available Electric Energy Flexibility ($AEEF$): This metric measures the variation of the building electrical energy consumption due to the activation of DR programs over a specific period τ. Defining P_{DR} and P_b as the electric power consumption profiles with and without DR actions respectively, the $AEEF$ can be expressed as follows:

$$AEEF^{(\tau)} = \int_0^\tau |P_{DR} - P_b| \cdot dt = \int_0^\tau |\alpha_{DR} - 1| \cdot P_b \cdot dt \tag{13}$$

- Primary Energy Efficiency (PEE): This metric is defined as the ratio between the primary energy consumption (PEC) with and without DR actions, as shown in Eq. 14. Since the activation of DR actions typically leads to higher primary energy consumption, PEE values lower than 1 can be expected. In this sense, the PEE provides quantitative information on the *energy cost* of the DR action.

$$PEE^{(\tau)} = \left(\frac{PEC_b}{PEC_{DR}}\right)_\tau \tag{14}$$

- Specific (Marginal) Costs (SC): The cost (C) associated with a specific DR program can be determined by comparing the system operational costs (OC) with and without the activation of the DR actions. The specific cost (SC) is therefore determined by the ratio between the total DR cost (C_{DR}) and the available energy flexibility provided ($AEEF$, Eq. 13):

$$SC_{DR}^{(\tau)} = \left(\frac{C_{DR}}{AEEF}\right)_\tau = \left(\frac{OC_{DR} - OC_b}{AEEF}\right)_\tau \tag{15}$$

These KPI will depend on the DR measure adopted and on its intensity and duration (Eq. 10 and Eq. 11). It is also important to highlight that proper optimised system controls should be adopted, as described in section 2.3, to detect the optimal control schedule in any scenario considered, thus to include possible control inefficiencies into the flexibility metrics.

2.5. Tariff structures

The prices for 2016 originate from the study by Schmidt et al. [30], where new electricity tariffs based on hypothetical policy changes in the German power market were introduced for domestic consumers. The tariff was created by using a typical residential demand profile and analysing which times of the day are the most expensive in terms of providing electricity to the customer. Based on different assumptions concerning the structure of taxes, network fees and surcharges (Table 3, [30]), different price scenarios were developed:

1. *Real Time Price* (RTP): starting from the EPEX SPOT market Schmidt et al. [30], dynamic retail prices are generated by considering the fixed price component shown in Table 3. The RTP profile generated can be seen in Figure 3a.
2. *Standard two-level Day/Night tariff* (DNT): this represents the currently available tariff structure for consumers. The higher tariff level occurs during the weekdays between 8:00 and 20:00 hrs, with the lower tariff occurring at all other times. The profile is the same for all weeks throughout the year (Figure 3b).
3. *Critical peak pricing* (CPP): this is an evolution of the two-level tariff calculated by grouping the hourly wholesale prices (EPEX Spot) for 2016, with average prices calculated for each hour of the day throughout the year. These averaged price levels were then divided into three levels (i.e., low, medium and high) and their respective hours. Two different CPP tariffs are considered:
   - *CPP with fixed feed-in tariff* (CPP-F): it is generated by assuming a constant feed-in tariff of €$63.54/MWh_e$, while the variable price component of the network fee is adjusted based on the total distribution grid load measured at the transformer station at the network border (CPP-F). This measurement was based on real data for a community in south-west Germany. The average load on the network per hour of the day was calculated and sorted, with the network fees being adjusted and grouped into hours of similar demand. Multiplicative factors to the standard level of the network fee were calculated by reducing the fixed portion of the network fee from €$75/year$ to €$40/year$. The remaining €35 was incorporated into the variable portion of the network fees. The multiplicative factors for the adjustment of the variable part off the network fees were set to be 0.30, 1.30 and 2.75 (low, medium, high variations). The network fee for a given hour is equal to the product of the network fee and the multiplicative factor for the network fee for that hour. There is no maximum constraint on the calculated network fee. As in the previous tariff, the weekend features a constant price at the lowest level. The resulting tariff profile is shown in Figure 3c. A detailed description on how to calculate the CPP-F tariff is reported in Schmidt et al. [30].
   - *CPP with variable feed-in tariff* (CPP-V): this is generated by altering the feed-in tariff from a constant value (see the CPP-F description above) to a fee that changes every hour. An average of EPEX Spot prices in a set time interval is scaled by one of three multiplicative factors depending on the level of the wholesale EPEX Spot prices. The resulting tariff was calculated such that the average

Price component (variable)	Price component (fixed)
Variable network fees	Fixed network fees
Variable sale margin retailer	Fixed sale margin retailer
Regulatory surcharges	Metering fees
Concession levy	
Electricity tax	
Wholesale energy costs	
Value-Added Tax (19%)	

Table 3: List of variable and fixed price components [30]

household customer pays the same contribution to the feed-in tariff over the whole year, while not accounting for potential demand response actions. The resulting average spot price tariffs are €23.10/MWh_e, €29.28/MWh_e and €34.17/MWh_e, with the respective multiplicative factors being 0.65, 1.90 and 3.55 (low, medium, high variations). The feed-in tariff is equal to the product of the spot price for the ToU level and the multiplicative factor for ToU level. A final constraint is placed on the maximum level of the feed-in tariff, with the maximum value being twice the original level of the feed-in tariff. The resulting tariff profile is shown in Figure 3d. A detailed description on how to calculate the CPP-V tariff is reported in Schmidt et al. [30].

3. Results

The present section reports the results obtained by the methodology described in section 2 over the 2016 winter season (October - April). The RTP profile was used to determine the activation of the demand response programs in accordance with the assumption described in section 2.5. The resulting activation schedule of the DR programs is directly linked to periods with high RTP as shown in Figure 4, where it can be observed that a similar pattern with two periods with RTP higher than the threshold occurs, one in the morning and one in the evening. Generally, a seasonal trend can be discerned from Figure 4, by observing that the evening events tend to occur later at the beginning and end of the heating season while, on the contrary, the morning DR events occur earlier. Moreover, it can be observed that several short-time high price events occur during the night. However, these events do not actually lead to any real DR events for the case study analysed in the present work, since they occur outside the building heated hours and therefore are neglected.

In order to describe in more detail, the different system schedules obtained by the MPC, the following sections outline the resulting optimisation schedule of the generators with and without the activation of the DR programs (section 3.1) and the influence of different ToU structure on the DR program techno-economic assessment (section 3.2).

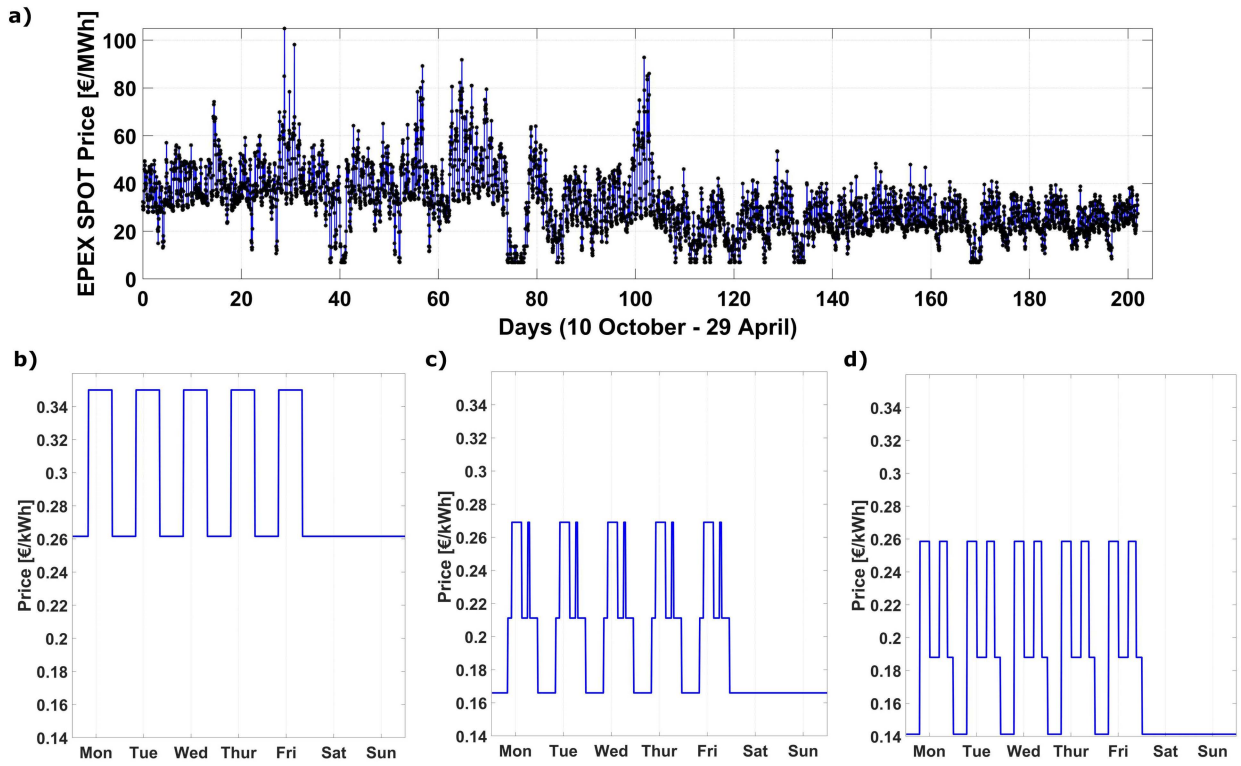

Figure 3: (a) EPEX SPOT retail price of electricity (RTP). ToU tariffs: (b) Two-level Day/Night tariff, (c) Critical peak pricing with fixed feed-in tariff (CPP-F), (d) Critical peak pricing with variable feed-in tariff (CPP-V) [30].

3.1. Optimised schedule under DR events

Figure 5 shows the comparison between the heat pump load share obtained by the MPC with and without DR programs. The baseline case without activated DR programs (Figure 5a) shows that the heat pump operates almost continuously through the winter season, with it being the main generator providing the heat demand required by the building. The maximum values of HP power occur early in the morning at the beginning of the comfort period, when the building must be reheated up to the set point temperature (22^oC). Moreover, it can be noted that the HP operates during short periods in the night, when no building demand occurs. Typically, cheaper electricity prices during the night make it more economically favourable to keep the TES fully charged (i.e., at its maximum temperature) and ready to be discharged as the daily building set point starts. When the DR programs are activated (Figure 4), a large change in the HP profile occurs, since the MPC forces the HP to stop operating (maximum intensity, $\alpha = 0$), as can be noted in Figure 5b. From one side, this leads to a reduction of the electricity load during these hours, while an increase of HP operation occurs with the aim of charging the TES before the DR action is implemented. This load increase may happen hours before the scheduled DR action, due to the time horizon of the MPC when minimising the operational cost of the hybrid system. This uncertainty leads to challenges in isolating the influence of each DR action during the techno-economic

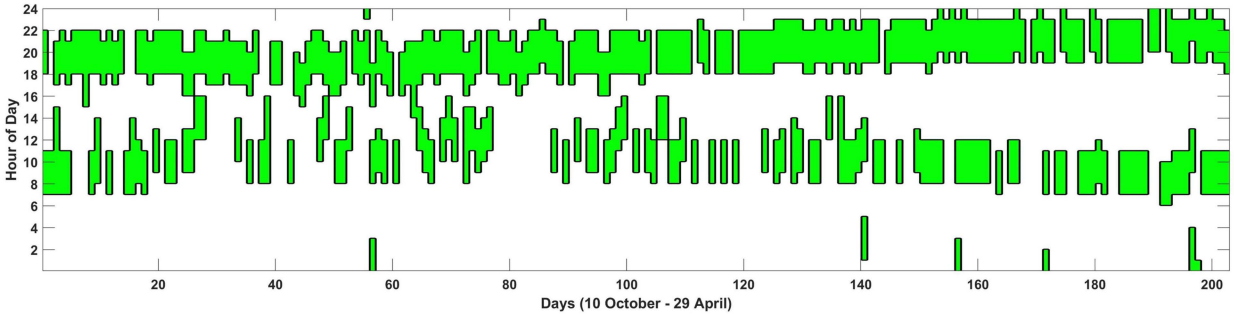

Figure 4: Times of DR events throughout heating season

assessment.

Generally, the installation of a TES alongside the generators increases the overall thermal inertia of the building energy system and consequently, its flexibility. Increasing the shifting potential allows the exploitation of the dynamic structure of the RTP; the TES is typically charged by the HP when the electricity price is low (i.e., night) and then discharged during peak price periods. This will allow significant cost savings despite a greater overall consumption due to the energy losses of the TES. This augmented thermal inertia provided by the TES is beneficial for DR program, since it allows decoupling of the energy system from the building demand which may enable a higher shifting potential with longer duration and higher intensity. This large exploitation of the TES obtained by activating the DR programs can be seen in Figure 6 which shows the maps of the TES discharging loads over the considered winter period.

On the other hand, the TES thermal inertia may not be sufficient to guarantee the building heating demand, especially during peak load periods. When this happens, the MPC is forced to use the boiler to cover the remaining load share. Figure 7 shows the boiler load share resulting from the optimised schedule over the considered winter period. It can be seen that for the baseline scenario (no activated DR programs), the boiler contribution is limited to small periods, mainly at the beginning of the heating hours, when the temperature set point needs to be restored (Figure 7a). On the other hand, the activation of DR programs leads to higher boiler consumption (Figure 7b, especially during the coldest months (December - February), when the TES is not capable of storing enough thermal energy to cover the building energy demand in the case of DR actions. Since the MPC performs a cost minimisation, both TES and boiler are used by switching from one to the other and with the priority given to the TES, while the boiler is used as backup at the end of the DR event.

Table 4 reports the seasonal results obtained from the different DR programs analysed. As a result of the optimised controller, the HP covers more than 96% of the overall building energy consumption for the baseline scenario while, limiting the boiler contribution and the exploitation of the TES. The implementation of DR programs leads to higher use of the TES and a greater boiler consumption, up to 17.1% and 12.1%, respectively in case of maximum DR intensity, which in turn leads to a higher overall primary energy consumption (PEC) and costs. Assessing these (marginal) costs is paramount to characterising the value and,

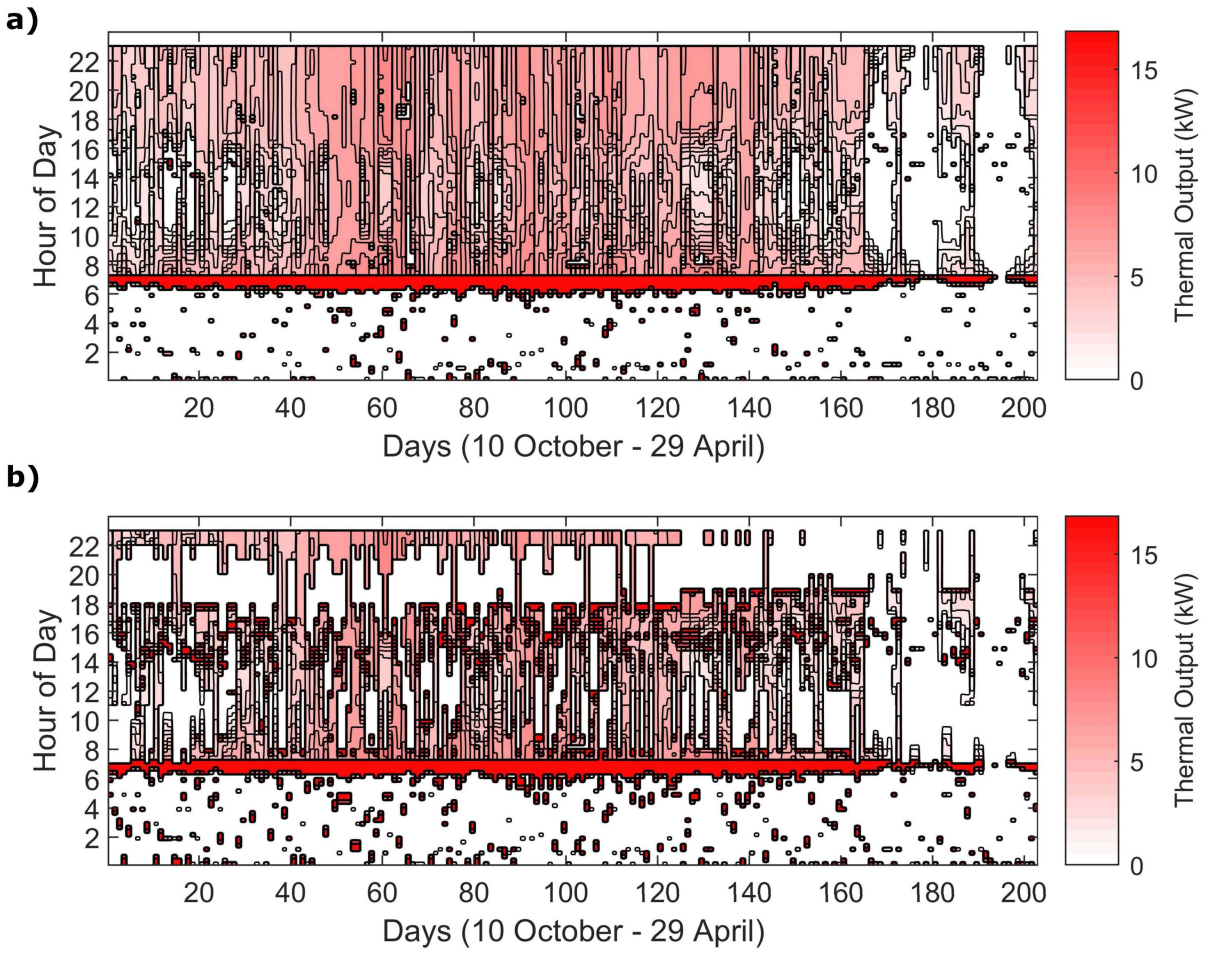

Figure 5: Map of the heat pump load over the heating season: (a) baseline without DR programs; (b) DR programs at maximum DR activation level.

therefore, the potential economic suitability of these DR programs in a hypothetical DR market. Generally, values up to 1370 kWh of AEEF can be achieved over the whole winter season with average specific costs between €0.024 - €0.035 per kWh of flexibility provided. However, an increase of the primary energy consumption (PEC), which was estimated to be between 1.6% and 9.1% depending on the event intensity, is observed. It can also be noted in Table 3 that, when the DR intensity is constrained to 50% of the partial load and duration, the TES is capable of covering most of the load shifting caused by the DR events, limiting the boiler usage to small percentages. This is also confirmed by the small reduction of the primary energy efficiency (PEE) values observed for partial load DR events.

3.2. Influence of the tariff structure

While the previous section analysed the changes in the operating conditions of the energy system due to the activation of DR programs, the present section investigates the influence of the different tariff structures (Figure 3) on the flexibility metrics described in section 2.3.

Scenario	**Load share**			**Overall**	**Specific**	**Flexibility metrics**		
	HP	Boiler	TES	**PEC**	**Cost**	AEEF	Cost	PEE
Units	%	%	%	kWh	€	kWh	€/kWh	-
Baseline	96.2	1.2	2.6	11,963	914.10	-	-	-
DR (max intensity)	70.8	12.1	17.1	13,048	962.30	1,370	0.035	0.91
DR (75% intensity)	79.5	4.0	16.6	12,453	935.80	787.15	0.028	0.96
DR (50% intensity)	89.7	1.8	8.5	12,159	922.45	358.5	0.023	0.98

Table 4: Seasonal comparison between different scenarios of DR programs under RTP market.

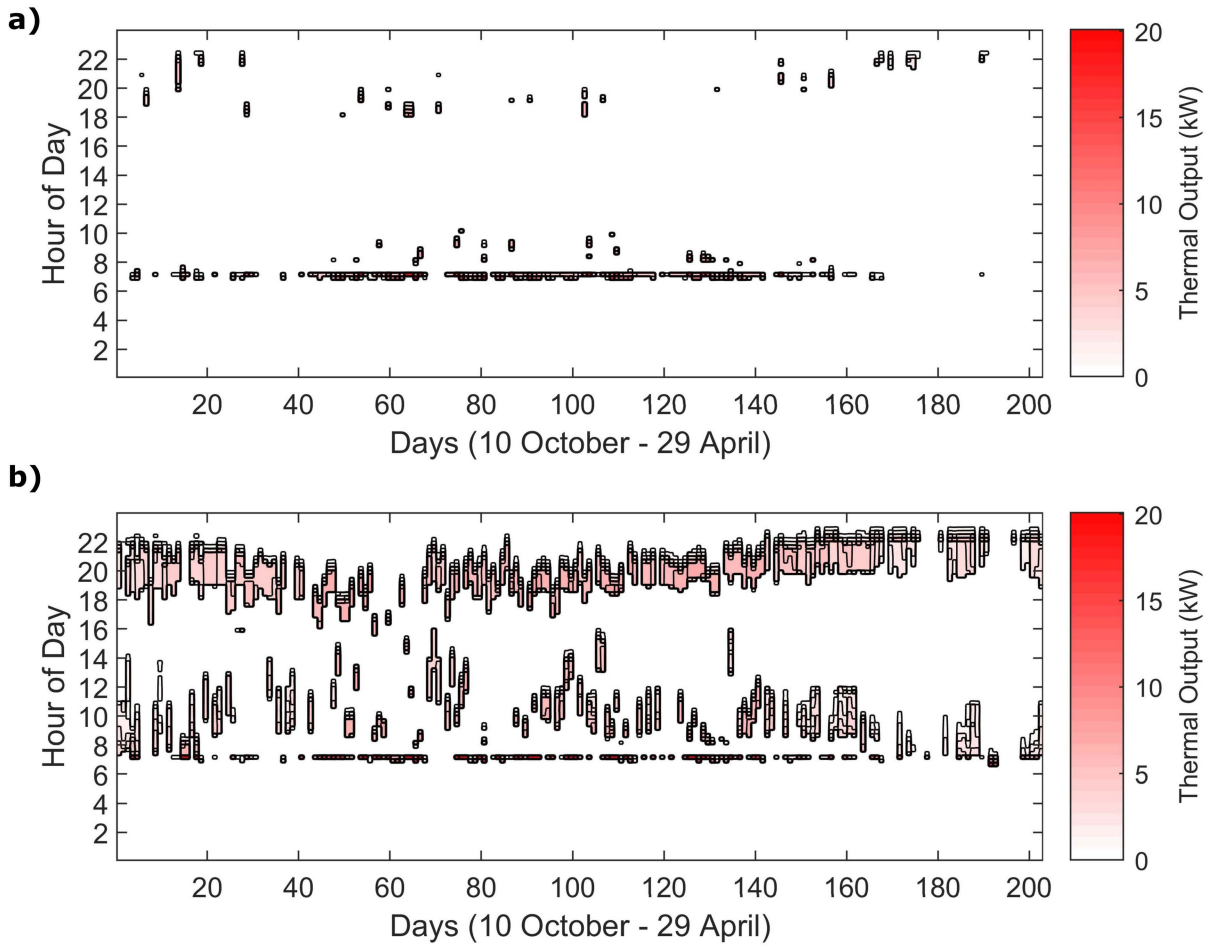

Figure 6: Map of the TES discharging loads over the heating season: (a) baseline without DR programs; (b) DR programs at maximum DR activation level.

Figure 8 shows the total seasonal electric energy flexibility available (AEEF) as function of the duration and intensity of DR actions under different tariff structures. From the AEEF point of view, the RTP represents the most favourable tariff structure (Figure 8a) compared to the other ones, leading to higher values of AEEF (up to $AEEF = 1370kWh$ as shown in Table 4) due to a better exploitation of the price volatility and RTP being the reference adopted for triggering the DR actions (see Figure 4). On the other hand, the two-level (day-night) tariff exhibits the worst performance in terms of AEEF over the evaluated season (Figure 8b). This can be explained by considering two aspects: the day-night tariff results in an overall price of the electricity higher than the other tariff structures (see Figure 3b), which results in a reduction of the operating hours of the HP in the baseline case (no DR programs), consequently, a lower potential of reducing the electricity consumption during DR programs. Moreover, the day-night structure is not capable of offering enough elasticity to the system for storing/shifting energy during the heating hours, due to the long and constant high peak value shown.

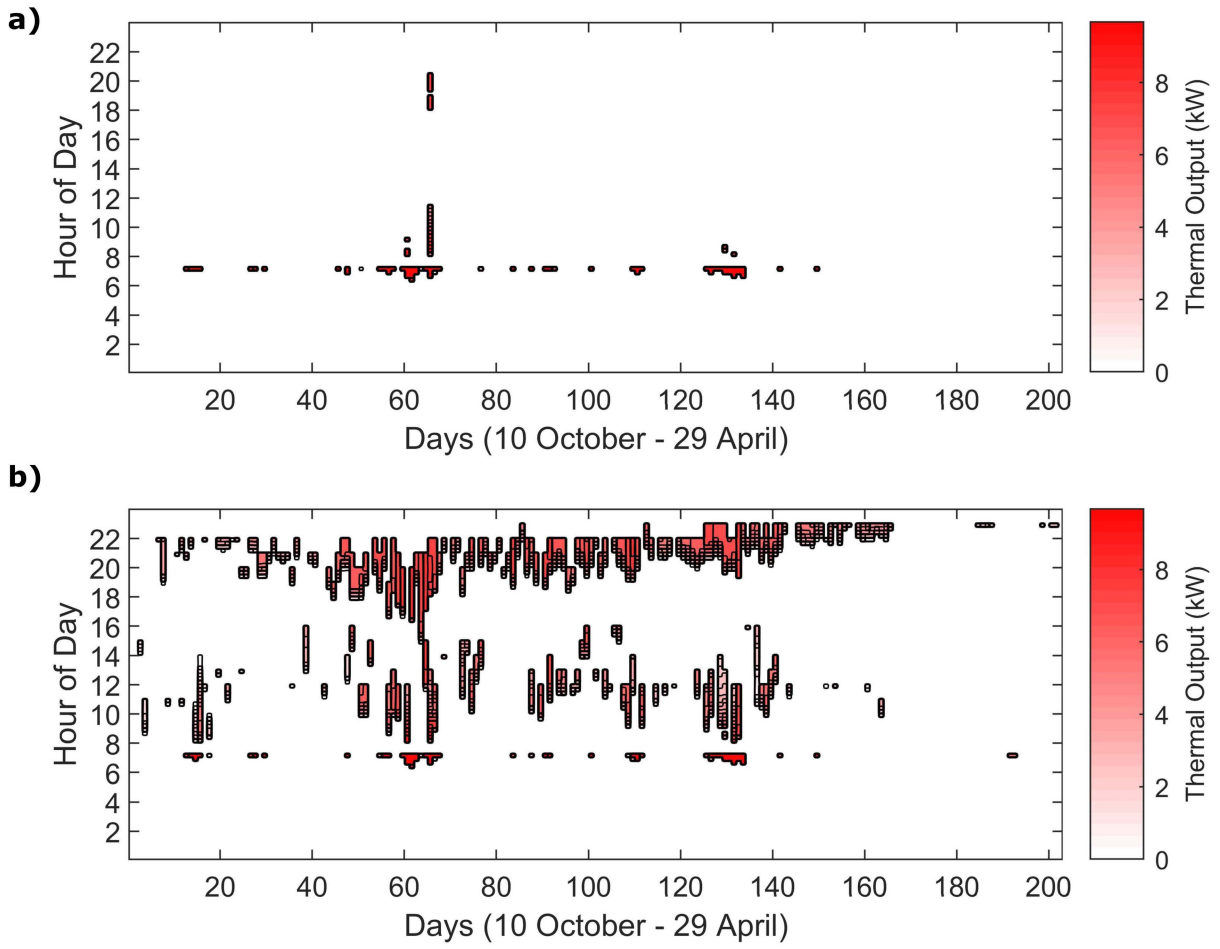

Figure 7: Map of the boiler loads over the heating season: (a) baseline without DR programs; (b) DR programs at maximum intensity activated.

Finally, it can be noted that the three-level tariff scenarios show different behaviours: while the CPP-F tariff (Figure 8c) can achieve AEEF values comparable with RTP ones (Figure 8a), lower values were obtained by using the CPP-V tariff. This can be related to the longer duration of the peak tariff periods which characterises the CPP-V tariffs compared to the CPP-F, which leads to a reduction of the HP usage in the baseline case with no DR actions implemented. These peak tariff periods tend to overlap with the DR events, which typically occur early in the morning and in the late afternoon/evening (see Figure 4), depending on the RTP. Since the AEEF is calculated referring to the baseline profile, a lower electric consumption in the latter means a reduction of the AEEF potential of the system.

The primary energy efficiency maps (Figure 9) show a general decrease with increasing duration and intensity of the DR measures for all tariff structures considered. This corresponds to increasing use of primary energy consumption while the building provides increasing amounts of flexibility to the grid. Generally, increasing amounts of AEEF (Figure

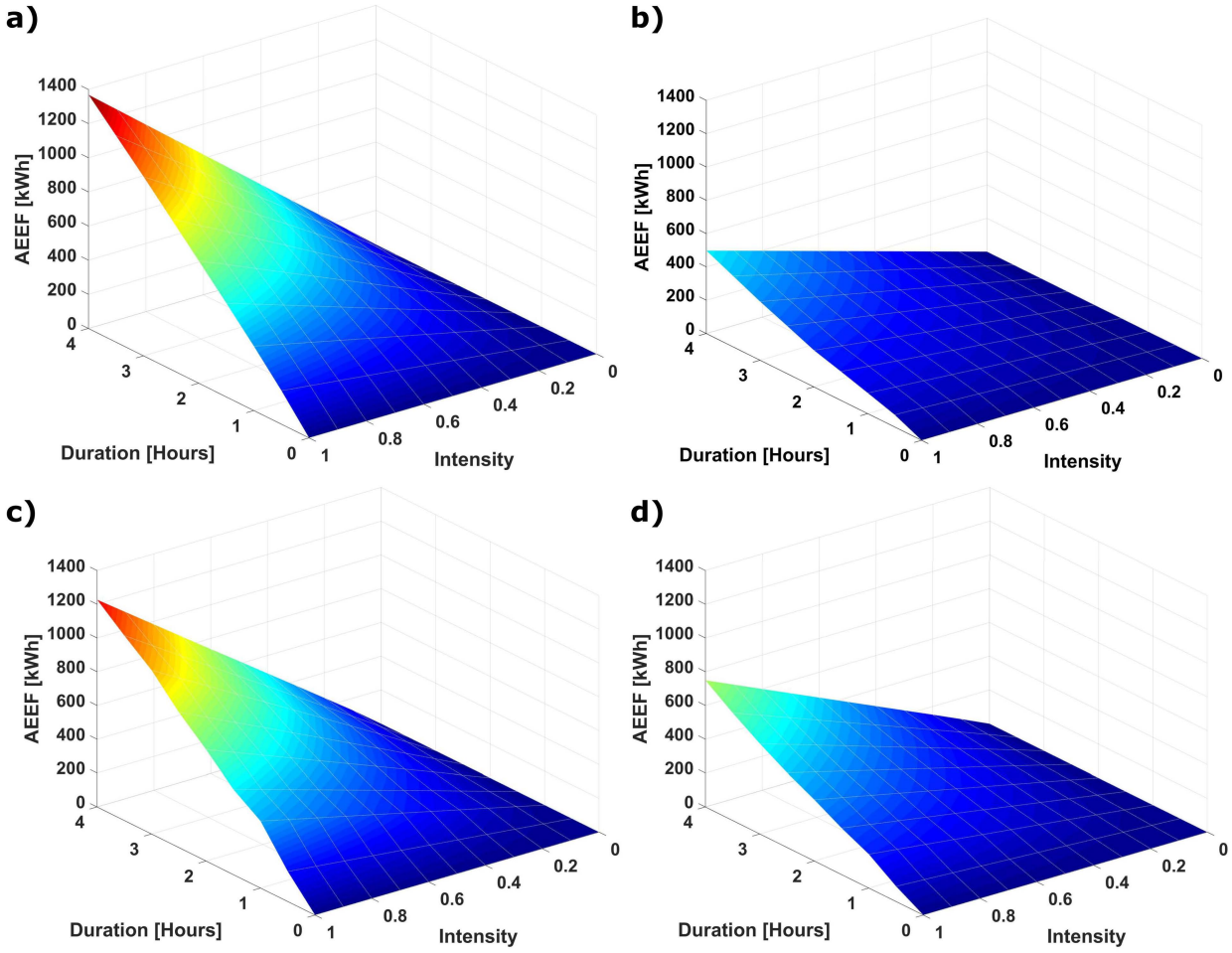

Figure 8: Maps of the Available Electric Energy Flexibility (AEEF) of the DR programs as function of the intensity and duration. End-user tariffs: a) RTP; b) Day-night tariff; c) Critical Peak Price with fixed feed-in tariff (CPP-F); d) Critical Peak Price with variable feed-in tariff (CPP-V).

8) corresponds with reductions in primary energy efficiency due to the increasing usage of the gas boiler and thermal storage to cover the building energy demand. Despite the greater consumption driven by the activation of DR programs, aggregating multiple load reduction profiles during high stress periods of the grid, can overall lead to better and more efficient operating conditions at the generation side. However, measuring the efficiency of DR actions at local (building) level, together with their costs, is paramount if a proper comparison between different measures is carried out with a decision-making perspective, especially if proper regulations and subsidies aimed at reducing the carbon footprint of such measures are in place.

Another important aspect of assessing DR programs is represented by determining their cost. The optimisation procedure described is based on the minimisation of the overall operating costs of the system for all scenarios analysed, including the baseline one without DR actions. Generally, the activation of DR programs represents a strong constraint added

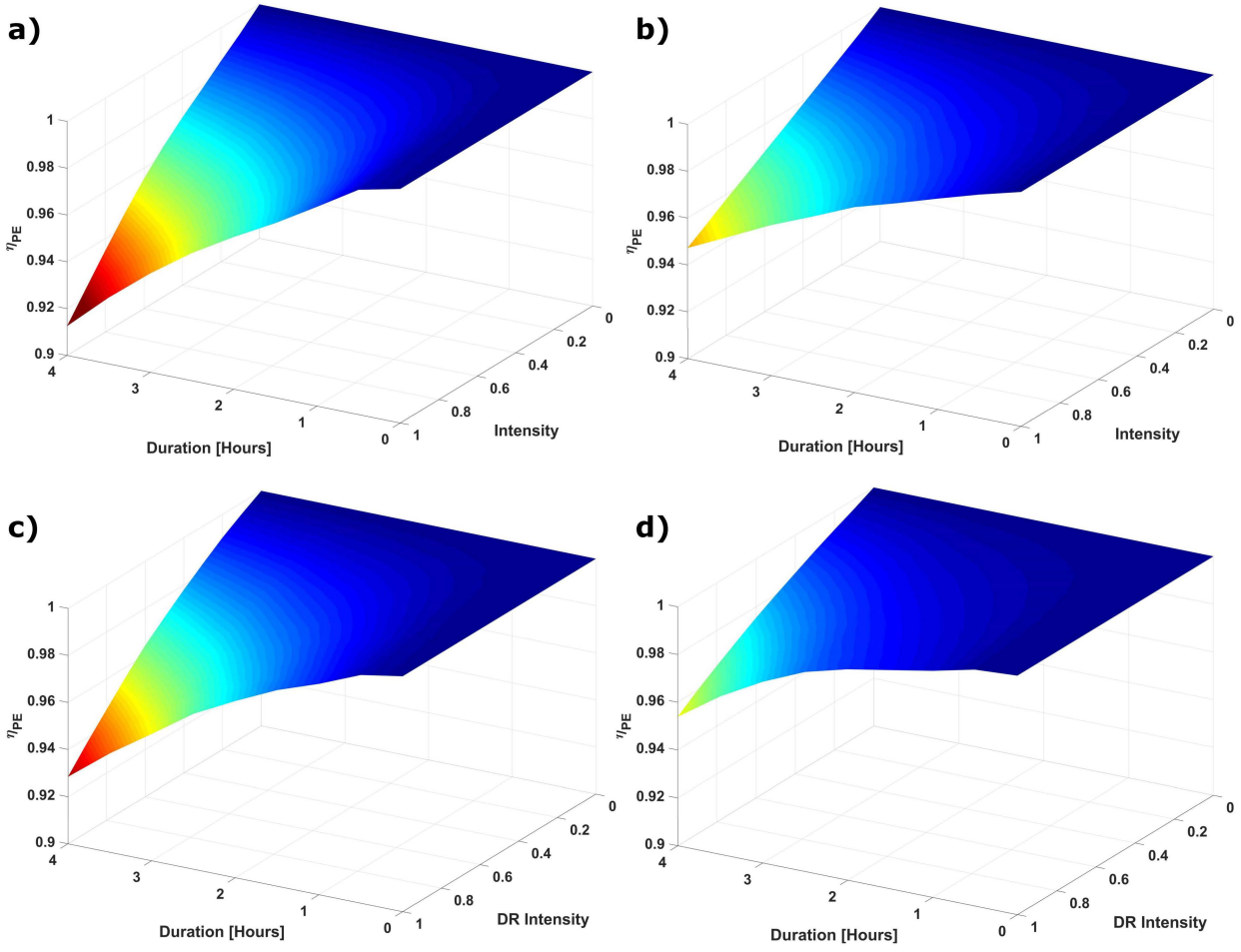

Figure 9: Maps of the Primary Energy Efficiency (PEE) of the DR programs as function of the intensity and duration. End-user tariffs: a) RTP; b) Day-night tariff; c) Critical Peak Price with fixed feed-in tariff (CPP-F); d) Critical Peak Price with variable feed-in tariff (CPP-V)

to the optimisation problem which, in turn, will lead to a sub-optimal (i.e., more expensive) operating schedule compared to the baseline case. In the present paper, these costs come from the greater boiler consumption and from the losses associated with the TES. Figure 10 shows the maps of the average seasonal specific cost of the DR actions over the heating season under the different tariff structures considered. It can be noted that shorter DR actions lead to lower specific cost due to the TES, which is capable of providing most of the required energy shifting during the DR action, limiting the contribution of the more expensive boiler. In this condition, the influence of different DR intensity values is limited. On the other hand, when longer DR actions are implemented, the TES storage capacity becomes insufficient to cover all the heat required during those actions and, therefore, a greater boiler consumption is required.

Comparing the different plots in Figure 10 in terms of the tariff structures considered, different behaviour can be seen. First of all, high variation of specific costs as function of DR

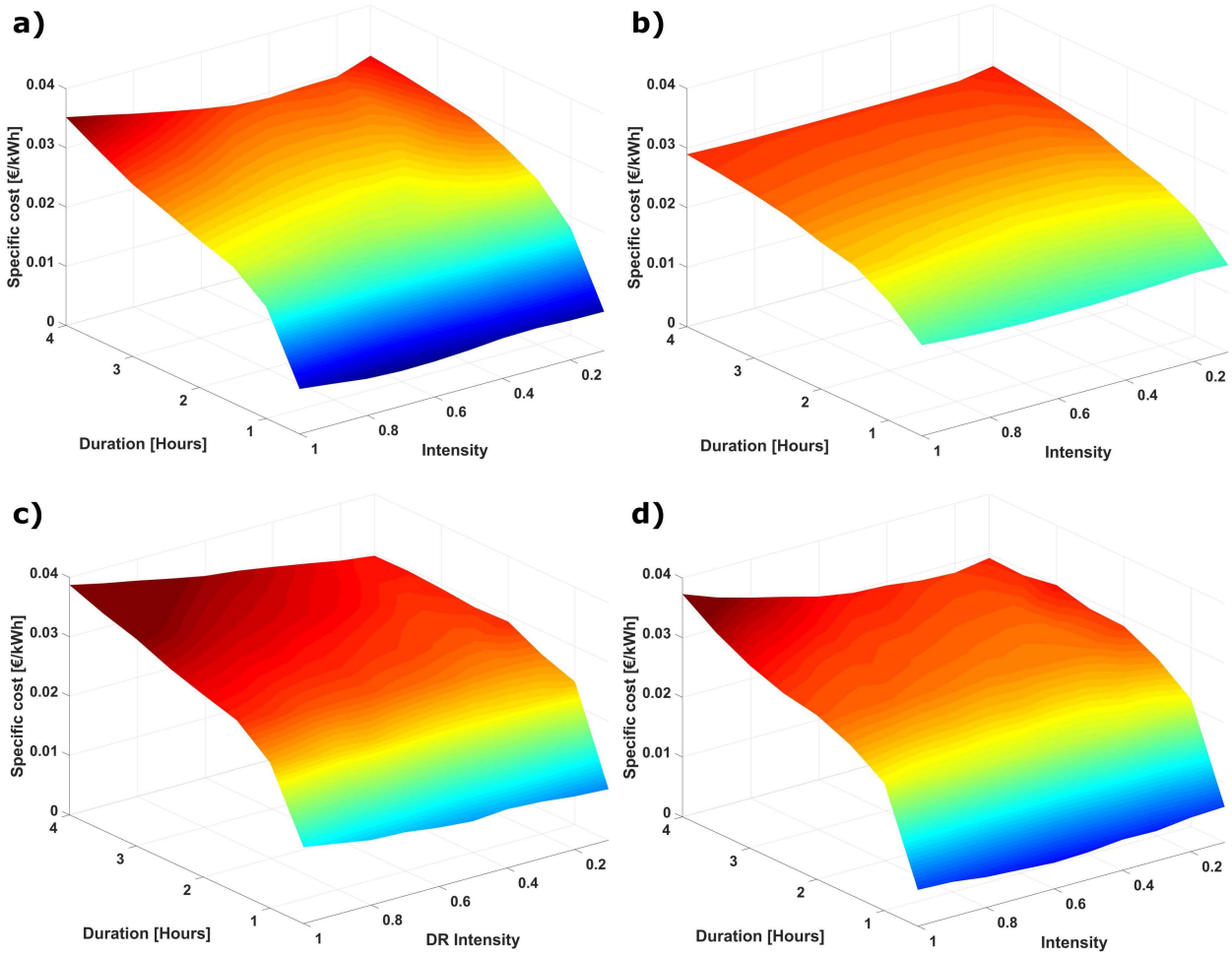

Figure 10: Maps of the specific cost of the DR programs as a function of the intensity and duration. End-user tariffs: a) RTP; b) Day-night tariff; c) Critical Peak Price with fixed feed-in tariff (CPP-F); d) Critical Peak Price with variable feed-in tariff (CPP-V)

intensity can be observed by the RTP structure (Figure 8a), the CCP-F (Figure 10c) and the CPP-V (Figure 10d) tariffs. Generally, the RTP structure is capable of offering higher values of AEEF (as shown in Figure 8a,c) with lower specific cost compared to the CPP-F tariff. Moreover, while a reduction of DR intensity leads to a decrease in the case of CPP-F, the RTP shows minimum values for a partial load reduction range of 40%-60%, depending on the DR duration. Furthermore, the CPP-V tariff structure (Figure 10d), shows similar profile to the RTP one, with lower values only for low DR intensity, despite the lower amount of AEEF provided (Figure 8d). Finally, the day-night tariff (Figure 10b) shows the lowest values of specific cost, with smooth variations as function of the DR intensity and duration, mainly due to the lack of flexibility potential of the tariff structure itself.

Starting from the seasonal maps shown before, Figure 11 shows the seasonal and daily average AEEF values for three DR intensity values under different tariff structures. Similar to the results shown in Figure 8, high daily AEEF values were obtained by the RTP and

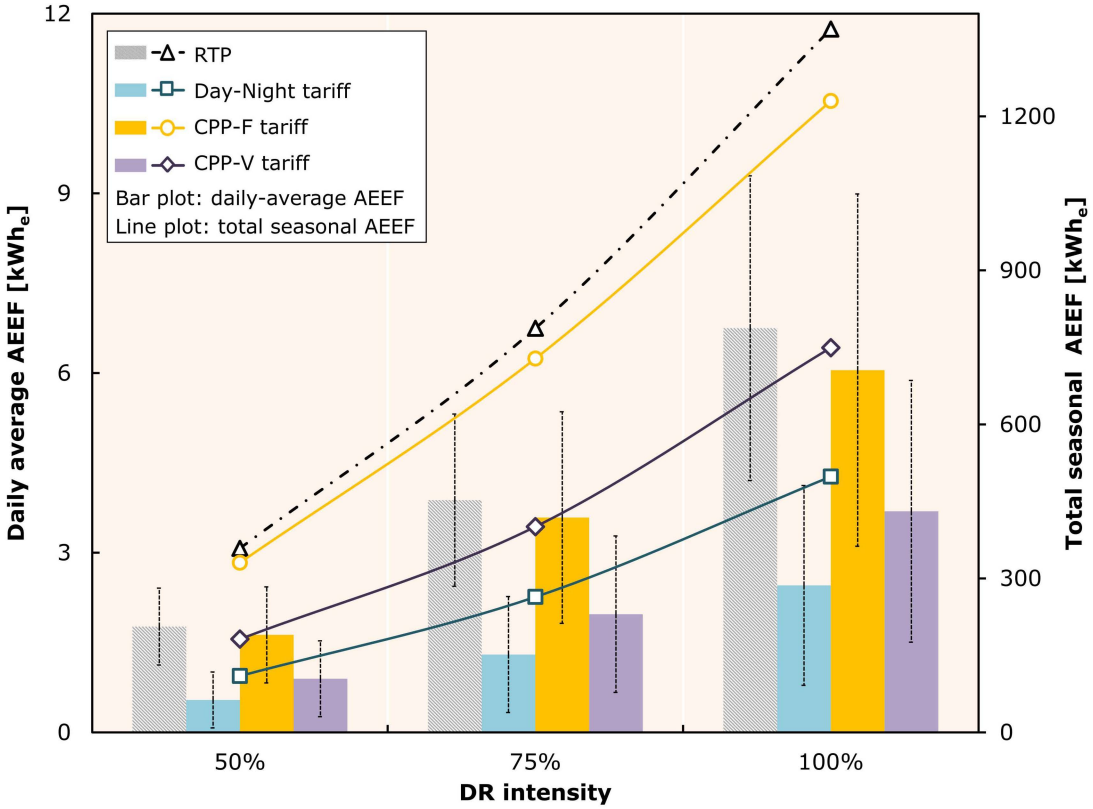

Figure 11: Daily-average and total seasonal AEEF in kWh_e as function of DR intensity and tariff structure (maximum DR duration = 4 hours).

CPP-F tariffs, with values up to 6.8 and 6.0 kWh_e for maximim intensity respectively, while low performances (daily AEEF lower than 3.5 kWh_e) were shown by the day-night and the CPP-V tariffs. Observing the error bars, which represent the confidence range of each daily values determined as standard deviations over the whole season, it can be noted that relative higher deviations occur. This can be explained by considering that these values were determined by analysing the whole heating season (October-April), with a consequent high variation of the climatic conditions which, in turn, affects the resulting energy flexibility.

Figure 12a shows the daily average specific (marginal) cost in €$/MWh_e$ for three values of DR intensity under the different tariff structures considered. First of all, it can be noted that the specific costs tend to rise with the increase of the DR intensity, in line with the results shown in Figure 10. Although the day-night and CPP-V tariffs are capable of offering a limited AEEF only (see Figure 8 and Figure 11), the marginal costs of this AEEF is lower compared to the other tariffs. On the other hand, the RTP tariff is capable of offering greater AEEF values at a lower price compared to the CPP-F, which resulted to be the most expensive tariff with marginal costs up to 33 €$/MWh_e$ for maximum intensity. As discussed for the AEEF values (Figure 11), since the analysis covers the whole heating season, high standard deviations were obtained for all daily average specific costs, with

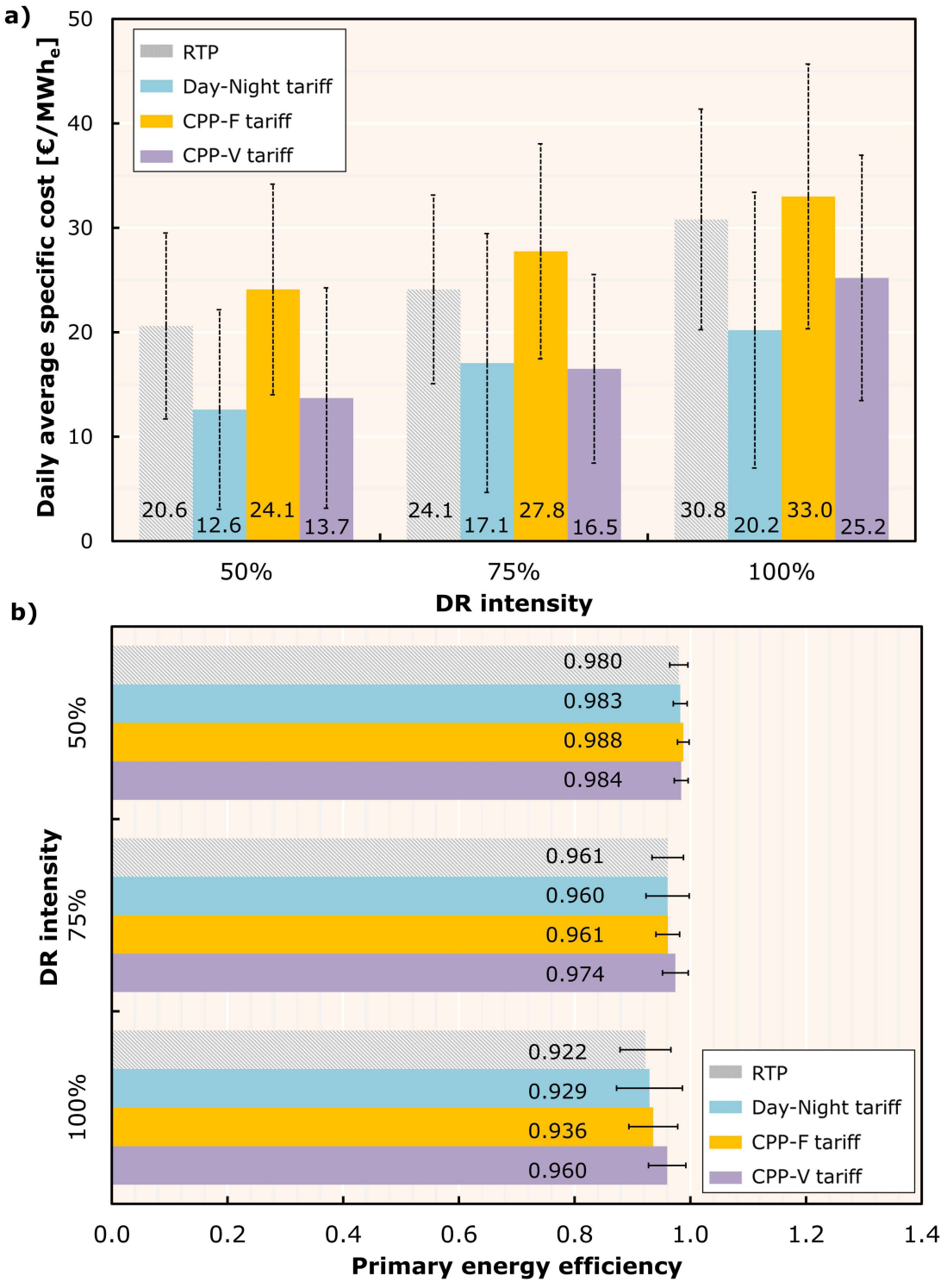

Figure 12: Daily-average specific cost in in $€/kWh_e$ (a) and primary energy efficiency (b) as function of DR intensity and tariff structure (maximum DR duration = 4 hours).

greater values for the day-night and CPP-V tariffs.

Similarly, Figure 12b shows the daily average PEE values, defined as shown in Eq. 14, obtained for three DR intensities and tariff structures. Values between 0.922 and 0.988 were obtained for all the tariffs analysed, a general decrease trend as function of the DR intensity. As already explained previously, increasing the DR intensity leads to a greater primary energy consumption due to the increase of boiler and TES usage. For lower DR intensity, most of the energy required during the DR action comes from what had been stored in the TES previously, less any thermal losses, which are responsible for the greater primary energy consumption shown. However, for higher DR intensities (i.e., 100%), the energy stored in the TES is not sufficient to cover all the heat required by the building during the DR action and, therefore, the boiler is forced to intervene with a consequent much higher primary energy consumption. This explains the drop shown by the PEE values in case of 100% DR intensity.

4. Conclusions

The aim of the present paper is to investigate the influence of energy market frameworks on building flexibility and associated energy costs. A residential building, a three-storey residential house located in Germany and equipped with a hybrid heat pump (HP) coupled with a thermal storage (TES) and a gas boiler, was selected as a test bed. A model predictive controller was used to optimise the daily operating schedule of the energy systems according to several time of use tariffs. Several demand response programs, based on switching the thermal load from the HP to the TES and boiler during peak-price periods, were tested under different tariff structures. The DR programs were assessed by introducing several metrics capable of describing the flexibility potential and energy cost of the adopted measures.

The results show that when no DR programs are activated, the heat pump operates almost continuously through the winter season, making it the main generator to meet the heat demand required by the building. However, when DR programs are activated, the controller forces the HP to stop operating. This leads to a reduction of the electricity load during these hours, but an increase to the overall HP operation, as the TES is charged before the DR action is implemented. This load increase may occur a number of hours before the scheduled DR action, due to the time horizon of the MPC when minimising the operational cost of the hybrid system. This uncertainty leads to challenges in isolating the influence of each DR action during the techno-economic and energy cost assessment.

Generally, the installation of a TES alongside the generators increases the overall thermal inertia of the building energy system and, consequently, its flexibility. The implementation of DR programs leads to higher use of the TES and a greater boiler consumption, up to 17.1% and 12.1%, respectively, in the case of maximum DR intensity, which in turn leads to higher overall primary energy consumption and costs. Assessing these (marginal) costs is paramount to characterise the value and, therefore, the potential economic suitability of these DR programs in a hypothetical DR market. Typically, values up to 1370 kWh of AEEF can be achieved over the whole winter season with average specific costs between €0.024 - €0.035 per kWh of flexibility provided. However, an increase of the primary energy

consumption, which was estimated to be between 1.6% and 9.1% depending on the event intensity, is observed.

The implementation of different tariff structures strongly influences the performance of the DR programs. Generally, the RTP is the most favourable tariff structure in terms of AEEF, showing seasonal values up to $AEEF = 1370kWh$, due to a better exploitation of the price volatility, as well as being the reference adopted for triggering the DR actions. The standard two-level (day-night) tariff exhibited the poorest AEEF performance over the season considered, due to the higher overall price of electricity compared to the other tariff structures, which makes the HP less effective. On the other hand, different behaviour was evident from the three-level tariff structure (CPP-F and CPP-V): the longer duration of the peak tariff periods, which characterises the CPP-V tariffs compared to the CPP-F, leads to a reduction of HP usage for the baseline case (no DR actions implemented). Since these peak periods tend to overlap with the DR events, lower AEEF values occur.

Generally, the activation of DR programs represent a strong constraint added to the optimisation problem which, in turn, will lead to a sub-optimal (i.e., more expensive) operating schedule compared to the baseline case. Shorter DR actions lead to lower specific costs due to the TES, which is capable of providing most of the required energy shifting during the DR action, limiting the contribution of the more expensive boiler. Typically, the RTP structure is capable of offering greater AEEF values at a cheaper price compared to the CPP-F, which resulted in the most expensive tariff with marginal costs up to 33 €$/MWh_e$ for maximum intensity.

Finally, from a Primary Energy Efficiency (PEE) perspective, a general decrease occurs with the activation of the DR programs for all tariff structures, due to the higher boiler share obtained, which is directly linked with the amount of AEEF generated. Despite this increment of the overall consumption, it is important to consider that aggregating multiple load reduction profiles during high stress periods of the grid, can ultimately lead to better and more efficient operating conditions on the generation side.

Although the results presented in the current paper refer to a specific building only, the methodology can be utilised for other building archetypes and has the potential to be scaled to aggregated building blocks. Heterogeneous building stocks could potentially be treated by adopting clustering techniques and by introducing stochastic models to take account of the variability associated with different user patterns, locations, markets and meteorological conditions. Future work is currently being carried out to extend the results presented in the paper with the aim to address the outstanding scalability and replicability challenges.

Acknowledgements

This work emanated from research conducted with the financial support of the European Commission through the H2020 project Sim4Blocks (Grant Agreement 695965) and of Science Foundation Ireland under the SFI Strategic Partnership Programme (Grant Number SFI/15/SPP/E3125).

Nomenclature

α	DR intensity
η	Efficiency
Φ	Load fraction
ϕ	Load factor
ρ	Density $[kgm^{-3}]$
τ	Time $[s]$
A	State matrix
ACH	Envelope leakage
$AEEF$	Available Electric Energy Flexibility $[kWh]$
B	Input matrix / Boiler
C	Costs [€]
c	Specific Heat $[Jkg^{-1}K^{-1}]$
COP	Coefficient of Performance
$CPP-F$	Critical Peak Price Tariff (Fixed)
$CPP-V$	Critical Peak Price Tariff (Variable)
DHW	Domestic Hot Water
DR	Demand Response
DSM	Demand Side Management
el	Electricity
F	Fixed
HP	Heat Pump
k	Discretised time
L	Load
l	DR duration $[h]$
MPC	Model Predictive Control

OC	Operational cost [€]
op	Operational
P	Electric Power $[W]$
p	Electricity/Gas price $[€kWh^{-1}]$
PEE	Primary Energy Efficency
PV	Photovoltaic
Q	Thermal Power $[W]$
RC	Resistance-Capacitance models
RTP	Real-Time Prices
SC	Specific cost $[€kWh^{-1}]$
T	Temperature $[K]$
t	time $[s]$
TES	Thermal Energy Storage
ToU	Time of Use tariffs
u	Control variable
V	Volume $[m^3]$
x	State variable
Z	Thermal Power (optimisation variable) $[W]$

References

[1] European Commission, 2030 climate and energy goals for a competitive, secure and low-carbon eu economy, `http://europa.eu/rapid/press-release_IP-14-54_en.htlm`, 2014. [last accessed: 10/07/2019].

[2] A. S. Brouwer, M. Van Den Broek, A. Seebregts, A. Faaij, Impacts of large-scale intermittent renewable energy sources on electricity systems, and how these can be modeled, Renewable and Sustainable Energy Reviews 33 (2014) 443–466.

[3] K. Klein, S. Herkel, H.-M. Henning, C. Felsmann, Load shifting using the heating and cooling system of an office building: Quantitative potential evaluation for different flexibility and storage options, Applied Energy 203 (2017) 917–937.

[4] F. D'Ettorre, M. De Rosa, P. Conti, D. Testi, D. Finn, Mapping the energy flexibility potential of single buildings equipped with optimally-controlled heat pump, gas boilers and thermal storage, Sustainable Cities and Society 50 (2019) 101689.

[5] T. Broeer, J. Fuller, F. Tuffner, D. Chassin, N. Djilali, Modeling framework and validation of a smart grid and demand response system for wind power integration, Applied Energy 113 (2014) 199–207.

[6] A. M. Carreiro, H. M. Jorge, C. H. Antunes, Energy management systems aggregators: A literature survey, Renewable and Sustainable Energy Reviews 73 (2017) 1160–1172.

[7] L. Gelazanskas, K. A. Gamage, Demand side management in smart grid: A review and proposals for future direction, Sustainable Cities and Society 11 (2014) 22 – 30.

[8] C.-L. Su, D. Kirschen, Quantifying the effect of demand response on electricity markets, IEEE Transactions on Power Systems 24 (2009) 1199–1207.

[9] P. Pinson, H. Madsen, et al., Benefits and challenges of electrical demand response: A critical review, Renewable and Sustainable Energy Reviews 39 (2014) 686–699.

[10] G. Schuitema, L. Ryan, C. Aravena, The consumer's role in flexible energy systems: An interdisciplinary approach to changing consumers' behavior, IEEE Power and Energy Magazine 15 (2017) 53–60.

[11] M. De Rosa, M. Carragher, D. P. Finn, Flexibility assessment of a combined heat-power system (chp) with energy storage under real-time energy price market framework, Thermal Science and Engineering Progress 8 (2018) 426 – 438.

[12] M. H. Shoreh, P. Siano, M. Shafie-khah, V. Loia, J. P. Catalão, A survey of industrial applications of demand response, Electric Power Systems Research 141 (2016) 31–49.

[13] S. Nan, M. Zhou, G. Li, Optimal residential community demand response scheduling in smart grid, Applied Energy 210 (2018) 1280–1289.

[14] IEA, Tracking Clean Energy Progress 2017, Technical Report, International Energy Agency, 2017.

[15] L. Park, Y. Jang, S. Cho, J. Kim, Residential demand response for renewable energy resources in smart grid systems, IEEE Transactions on Industrial Informatics (2017).

[16] F. Pallonetto, E. Mangina, F. Milano, D. P. Finn, Simapi, a smartgrid co-simulation software platform for benchmarking building control algorithms, SoftwareX 9 (2019) 271 – 281.

[17] M. Miara, D. Günther, Z. L. Leitner, J. Wapler, Simulation of an air-to-water heat pump system to evaluate the impact of demand-side-management measures on efficiency and load-shifting potential, Energy technology 2 (2014) 90–99.

[18] F. Pallonetto, E. Mangina, D. Finn, F. Wang, A. Wang, A restful api to control a energy plus smart grid-ready residential building: Demo abstract, in: Proceedings of the 1st ACM Conference on Embedded Systems for Energy-Efficient Buildings, BuildSys '14, ACM, New York, NY, USA, 2014, pp. 180–181.

[19] D. P. Chassin, J. Stoustrup, P. Agathoklis, N. Djilali, A new thermostat for real-time price demand response: Cost, comfort and energy impacts of discrete-time control without deadband, Applied Energy 155 (2015) 816 – 825.

[20] F. Pallonetto, M. De Rosa, F. Milano, D. P. Finn, Demand response algorithms for smart-grid ready residential buildings using machine learning models, Applied Energy 239 (2019) 1265 – 1282.

[21] D. Jang, J. Eom, M. J. Park, J. J. Rho, Variability of electricity load patterns and its effect on demand response: A critical peak pricing experiment on korean commercial and industrial customers, Energy Policy 88 (2016) 11–26.

[22] S. Nolan, M. OMalley, Challenges and barriers to demand response deployment and evaluation, Applied Energy 152 (2015) 1 – 10.

[23] S. Ruester, S. Schwenen, C. Batlle, I. Prez-Arriaga, From distribution networks to smart distribution systems: Rethinking the regulation of european electricity dsos, Utilities Policy 31 (2014) 229 – 237.

[24] E. Cutter, C. Woo, F. Kahrl, A. Taylor, Maximizing the value of responsive load, The Electricity Journal 25 (2012) 6 – 16.

[25] F. Pallonetto, S. Oxizidis, F. Milano, D. Finn, The effect of time-of-use tariffs on the demand response flexibility of an all-electric smart-grid-ready dwelling, Energy and Buildings 128 (2016) 56 – 67.

[26] L. Zhang, N. Good, P. Mancarella, Building-to-grid flexibility: Modelling and assessment metrics for residential demand response from heat pump aggregations, Applied Energy 233-234 (2019) 709 – 723.

[27] S. stergaard Jensen, A. Marszal-Pomianowska, R. Lollini, W. Pasut, A. Knotzer, P. Engelmann, A. Stafford, G. Reynders, Iea ebc annex 67 energy flexible buildings, Energy and Buildings 155 (2017) 25 – 34.

[28] R. G. Junker, A. G. Azar, R. A. Lopes, K. B. Lindberg, G. Reynders, R. Relan, H. Madsen, Characterizing the energy flexibility of buildings and districts, Applied Energy 225 (2018) 175 – 182.

[29] M. De Rosa, M. Brennenstuhl, C. Andrade Cabrera, U. Eicker, D. P. Finn, An iterative methodology for model complexity reduction in residential building simulation, Energies 12 (2019) 2448.

[30] J. Schmidt, M. Yadack, U. Eicker, Regulatory uncertainty and simulations of novel electricity tariffs for households: Applications in germany and demand elasticity, in: 2018 IEEE International Conference on Engineering, Technology and Innovation (ICE/ITMC), IEEE, pp. 1–7.

[31] M. De Rosa, V. Bianco, F. Scarpa, L. A. Tagliafico, Impact of wall discretization on the modeling of heating/cooling energy consumption of residential buildings, Energy Efficiency 9 (2016) 95–108.

[32] J. Löfberg, Yalmip toolbox, 2017. `https://yalmip.github.io/`.

[33] F. Scarpa, L. A. Tagliafico, V. Bianco, Inverse cycles modeling without refrigerantproperty specification, International Journal of Refrigeration 36 (2013) 1716 – 1729.